ADVANCED FUNCTIONAL MATERIALS

Supporting Information

for *Adv. Funct. Mater.*, DOI: 10.1002/adfm.201803969

Functional Peptide Nanofibers with Unique Tumor Targeting and Enzyme-Induced Local Retention Properties

*Vanessa Bellat, Richard Ting, Teresa L. Southard, Linda Vahdat, Henrik Molina, Joseph Fernandez, Omer Aras, Tracy Stokol, and Benedict Law**

Supporting Information

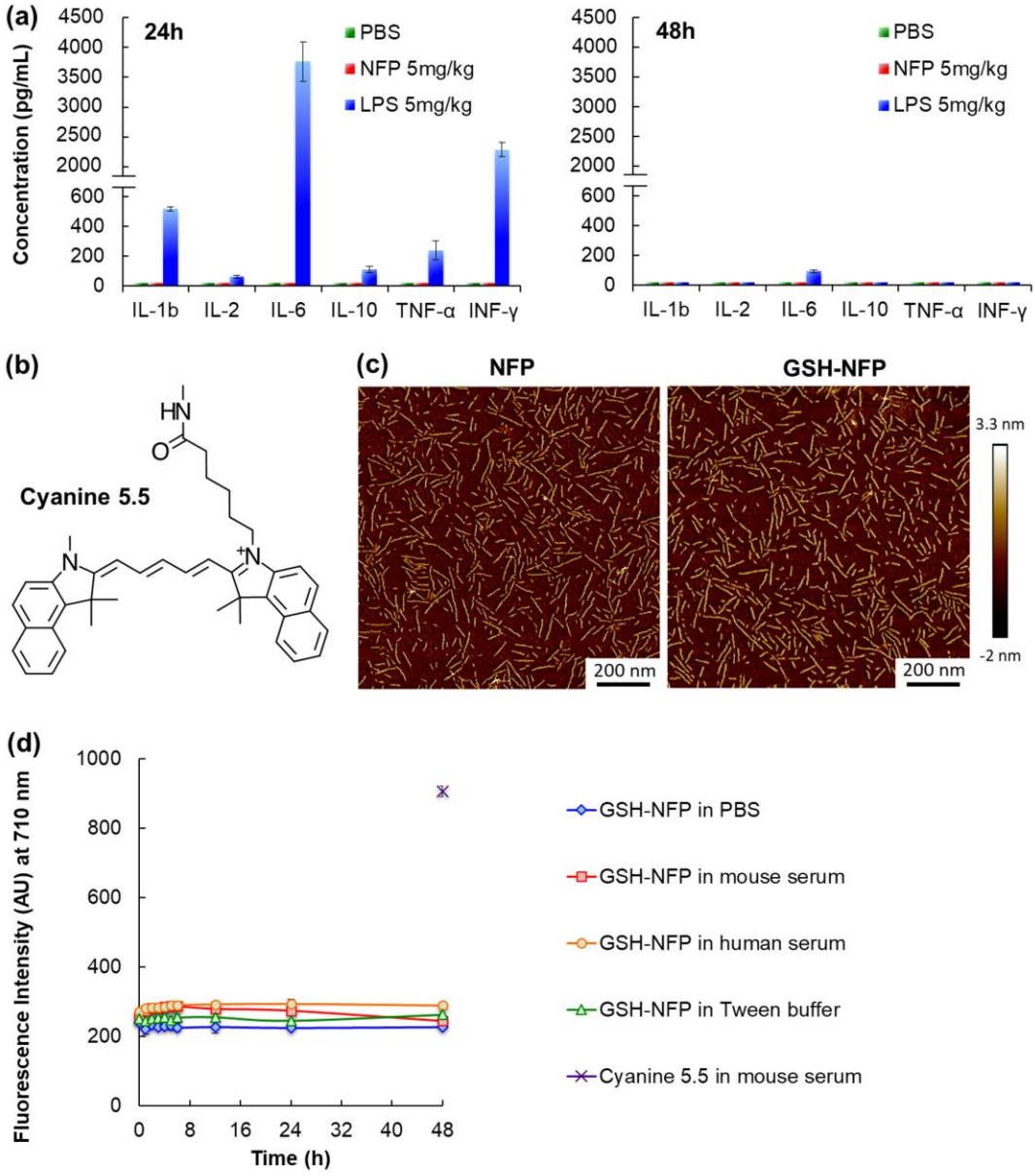

Figure S1: (a) The naïve NFP, assembled from $mPEG_{2000}$-KLDLKLDLKLDL-$CONH_2$, did not trigger innate immune response. The concentrations of cytokines (IL-1β, IL-2, IL-6, IL-10, TNF-α, and INF-γ) in the sera of female Balb/c mice (n=3) were measured with commercial sandwich enzyme-linked immunosorbent assay kits (Invitrogen, Carlsbad, CA) 24 and 48 h after IV injection of the nanofiber (5 mg/kg). Lipopolysaccharide (LPS, 5 mg/kg) and PBS were used as a

positive and negative control, respectively. (b) The chemical structure of Cyanine5.5, a near infrared fluorophore that was incorporated into a peptide construct for screening the tumoral uptake of the assembled nanofiber analogues. (c) AFM images of naïve NFP and GSH-NFP. The advanced nanofibers supplemented with GSH showed a similar morphology compared to naïve NFP. (d) A quenched version of GSH-NFP (co-assembled from a mixture of $mPEG_{2000}$-KLDLKLDLKLDLK-(Cyanine5.5), $mPEG_{2000}$-KLDLKLDLKLDLK-(GSH), and $mPEG_{2000}$-KLDLKLDLKLDLC in a ratio of 1:2:7) was prepared for studying the stability of the nanofiber (0.1 μM of fluorophore content). A plot of the fluorescence intensity confirmed that the nanofiber was stable (did not dissociate) in human and mouse sera, PBS, and Tween in PBS (1% w/w), as there was no dequenching of the fluorescence.

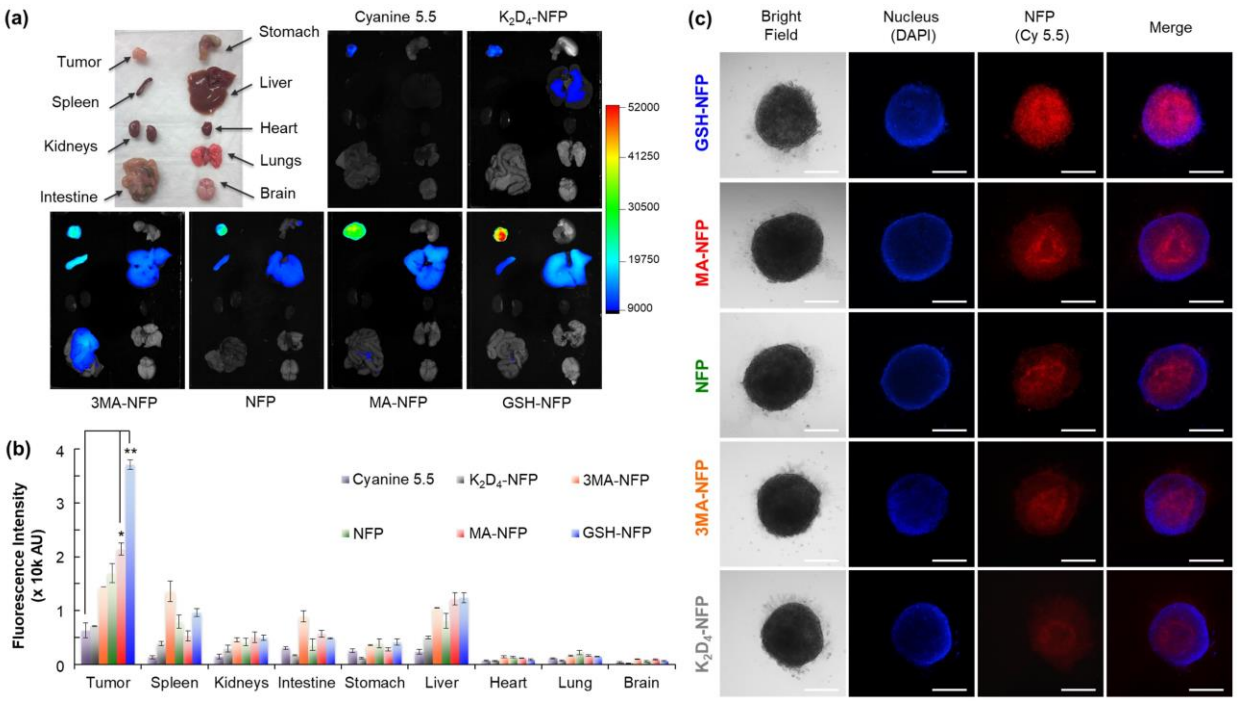

Figure S2: (a) The tumor-preferential distribution of GSH-NFP was confirmed by ex vivo imaging of the excised tumors and organs collected from animals euthanized 48 h after nanofiber injection. Representative photos and fluorescence images of tumors and organs. (b) The fluorescence intensity measured in the excised tumors and organs were plotted to compare the biodistribution of the NFP analogues. (*P<0.05, **P<0.01). (c) Compared to other analogues, GSH-NFP was more efficient in penetrating 3D cellular aggregates due to its higher negatively charged surface. Microscopic images of MDA-MB-468 spheroids incubated with NFP analogues (10 μM of peptide content) for 1 h. The bar scale represents 200 μm.

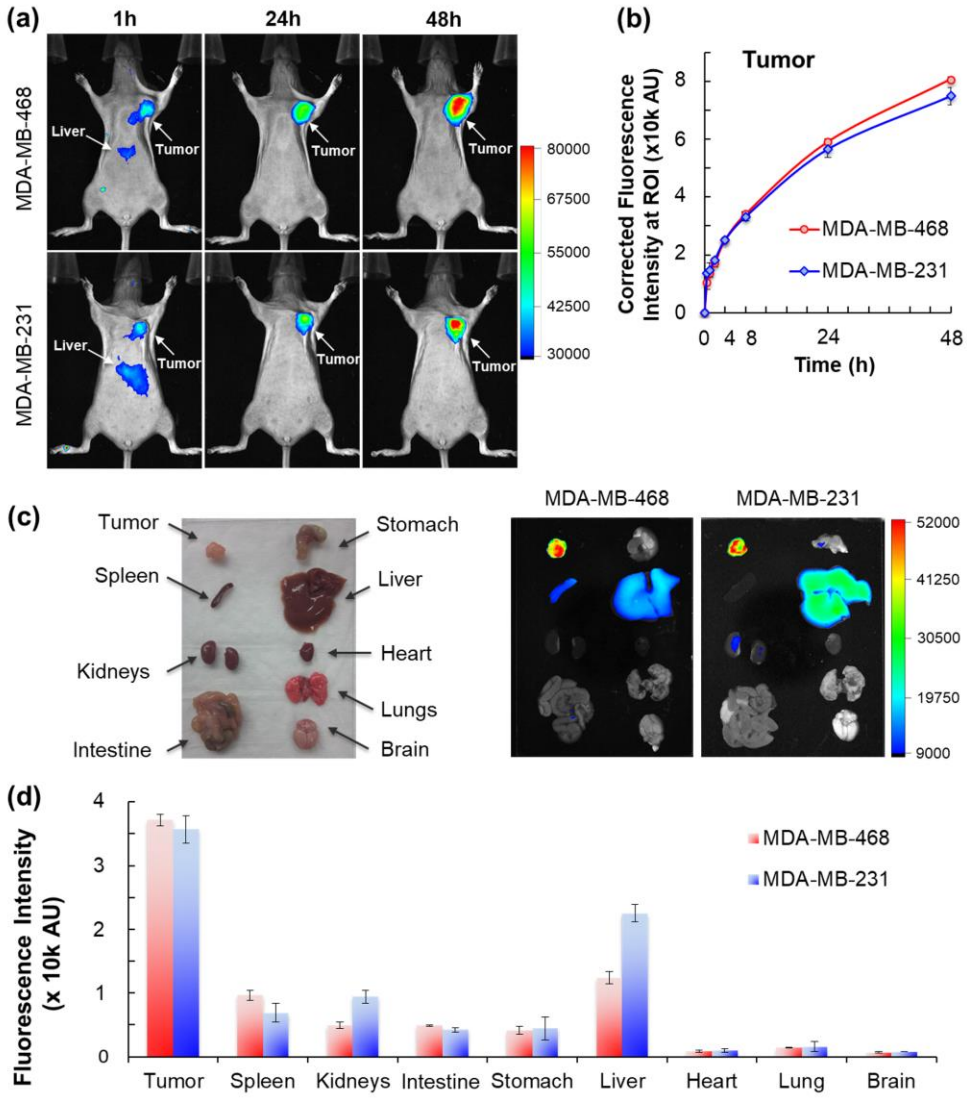

Figure S3: (a) In addition to the MDA-MB-468 tumors, GSH-NFP could also be taken up by other tumors such as MDA-MB-231. Whole body fluorescence images were acquired at various time intervals after IV injection of GSH-NFP (0.5 nmol of fluorophore content) into SCID mice bearing the tumors (n=3/group). (b) Plot of fluorescence intensity at the region of interest (ROI; tumor) showed a similar kinetic uptake in animals bearing MDA-MB-231 or MDA-MB-468 tumors. (c) Representative photograph and fluorescence images of the organs isolated from the animals euthanized after the *in vivo* imaging study. (d) Biodistribution of GSH-NFP based on fluorescence intensity measured in organs and tumors excised 48 h after nanofiber injection.

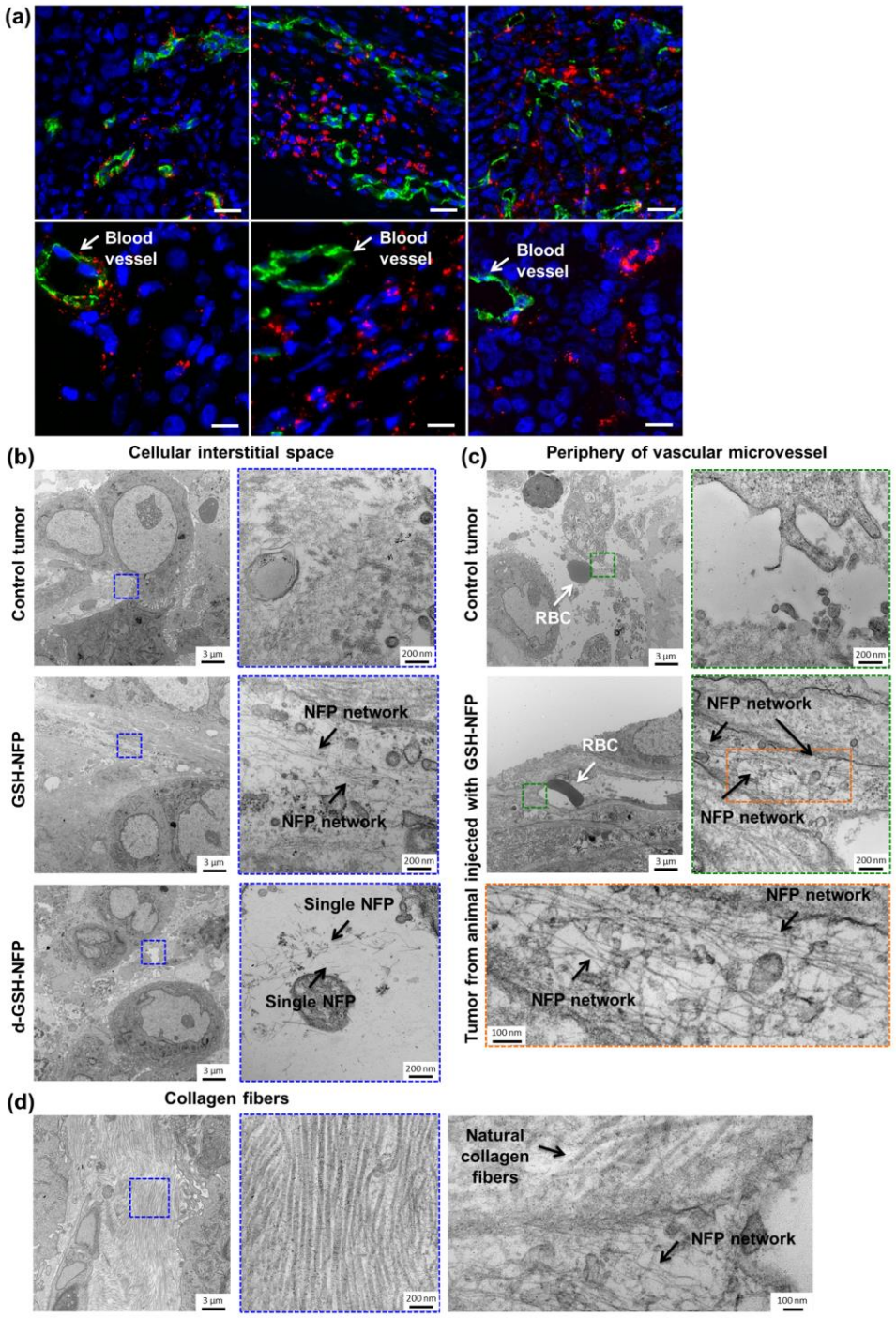

Figure S4: (a) Representative normal epifluorescence images of the tumor sections collected 12, 48, and 120 h after IV injection of GSH-NFP (5 nmol of fluorophore content) to the mice bearing MDA-MB-468 tumors. The nanofibers (red) were able to escape from the blood vessel and infiltrate the cancerous tissues. The blood vessels and cellular nucleus were stained with CD31

(green) and DAPI (blue) respectively. The scale bars represent 50 μm (top panel) and 10 μm (bottom panel). (b) Compared to the tumors of mice that were intravenously injected with GSH-NFP, we could not find the formation of interfibril networks in the interstitial spaces of the tumors from animals injected with either PBS (n=3) or d-GSH-NFP (also see TEM analysis in Figure 3f in the main text). (c) TEM analysis of the tumors from animals injected with GSH-NFP (100 nm, 200 nmol of peptide content) showed that the nanofibers transformed into networks at the periphery of microvessels. White arrows show a red blood cell inside the vessel while the black arrows indicate the presence of interfibril networks. We did not find these aggregated structures around the tumoral microvessels of control tumors (injected with PBS). (d) TEM images showing the morphological and structural differences between natural collagen fibers and the multiple nanofibers interfibril networks.

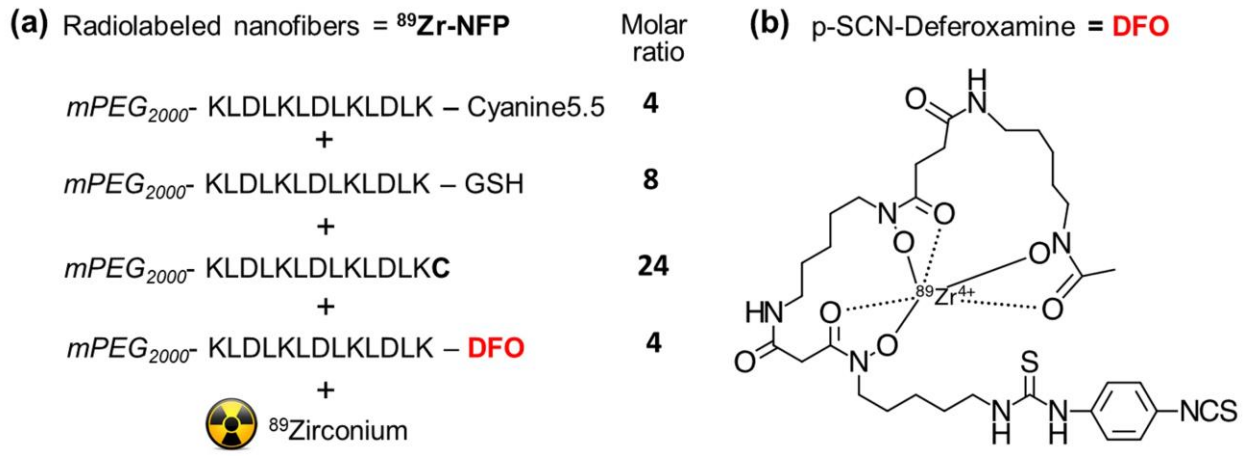

Figure S5: Synthesis of a dual Cyanine5.5- and ^{89}Zr-labeled GSH-NFP (^{89}Zr-NFP) for studying the biodistribution by fluorescence/PET/CT imaging. (a) The ratio of different peptide constructs used for assembling ^{89}Zr-NFP. Deferoxamine (DFO) served as the chelator of ^{89}Zr. (b) Molecular structure of DFO.

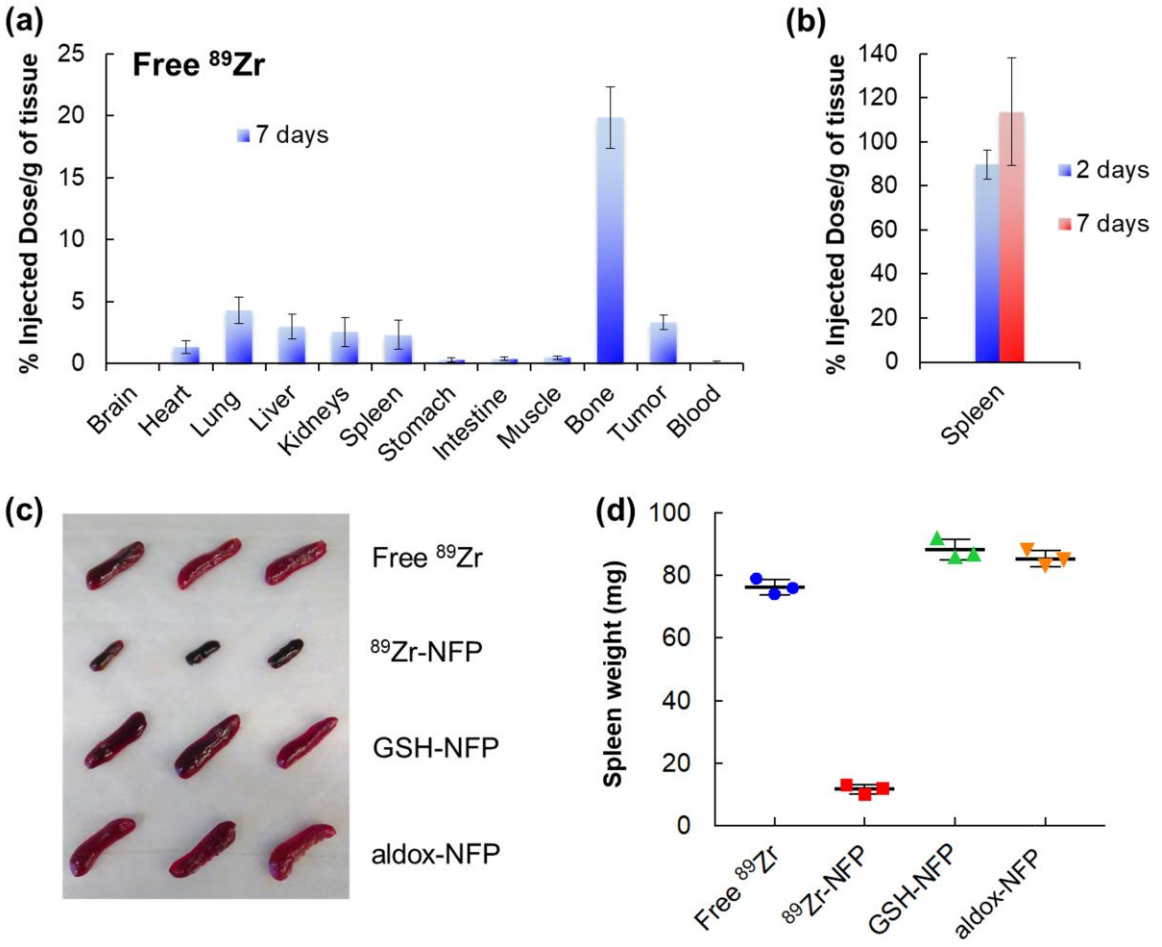

Figure S6: (a) Unlike ^{89}Zr-NFP, free ^{89}Zr-oxylate mainly distributed to the bones of SCID mice bearing MDA-MB-468 tumors after IV injection (n=4). The biodistribution of ^{89}Zr was expressed as % ID/g. The inclusion of ^{89}Zr-oxylate alongside the ^{89}Zr-NFP imaging data (Figure 4h in the main text) shows that minimal ^{89}Zr-ion dissociates from the ^{89}Zr-NFP-desferoxamine chelate. (b) ^{89}Zr-NFP showed abnormally high percentage of ID/g in the spleens. The spleens were collected from SCID mice bearing MDA-MB-468 tumors 2 or 7 days after injection of the nanofiber (n=4/group). (c) The high calculated ID/g in the spleens caused a marked reduction in splenic size 7 days after injection of ^{89}Zr-NFP. (d) Average weight of the spleens isolated from animals injected with ^{89}Zr-NFP was significantly less than animals treated with PBS (control), GSH-NFP, free ^{89}Zr, and doxorubicin-loaded NFP (aldox-NFP).

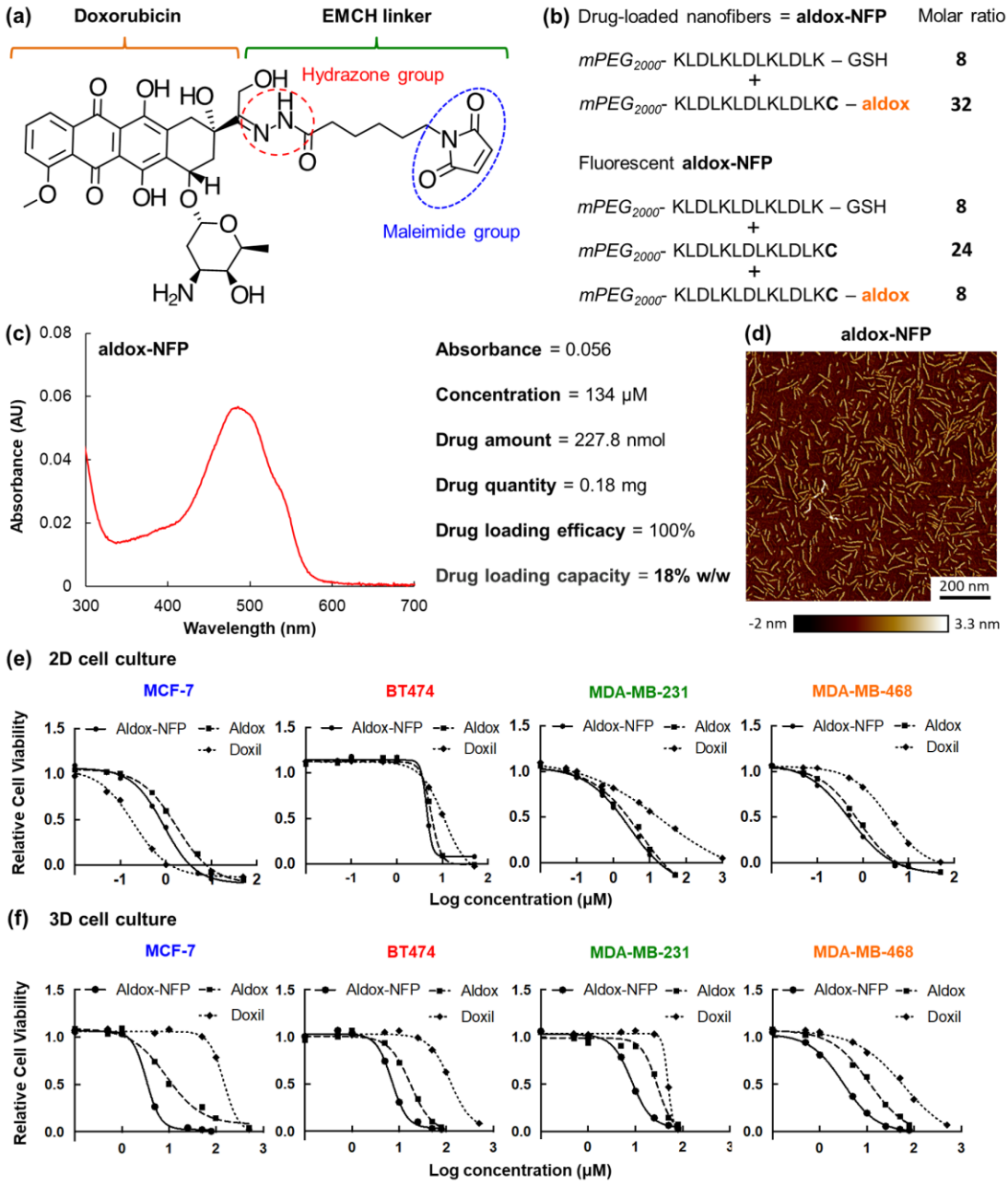

Figure S7: (a) Molecular structure of aldoxorubicin (aldox), a tumor-targeted doxorubicin conjugate containing an acid-sensitive cleavable hydrazone linker. (b) The ratio of different peptide constructs used for assembling aldox-NFP and fluorescent aldox-NFP. (c) UV absorbance spectrum of aldox-NFP. Measurement was performed in 5% (v/v) PBS in methanol and the maximum absorption λ_{max} of aldox was 495 nm. (d) AFM image of aldox-NFP. The

conjugation of the drug did not alter the morphology of the nanofiber. (e) Aldox-NFP displays a cytotoxic effect comparable to free aldox against different human breast cancer cell lines cultured in 2D. (f) In contrast, aldox-NFP is significantly more potent than Doxil when tested in 3D single-tumor spheroids. For both experiments, different concentrations of nanofibers or drugs (based on the doxorubicin content) were incubated with MCF-7, BT474, MDA-MB-231, and MDA-MB-468 2D cell lines or 3D tumor spheroids. After 72 h, cell viability was measured using the CellTiter-Glo Luminescent assay. All experiments were performed in triplicate.

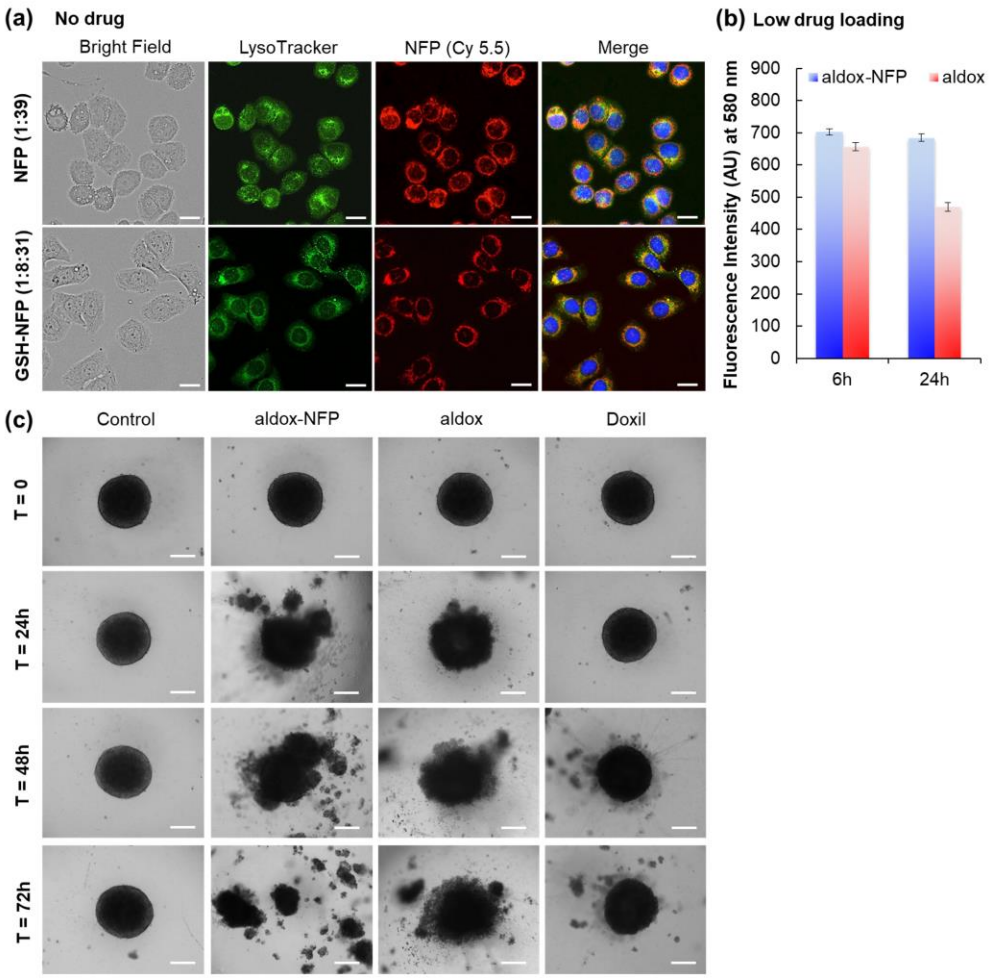

Figure S8: (a) Both naïve NFP and GSH-NFP (red) could be taken up by MDA-MB-468 cancer cells. Bright field and fluorescence images were acquired 6 h after incubation of the nanofibers (10 μM of peptide content). DAPI (blue) and LysoTracker (green) were used for nuclear and organelle staining. The bar scale is 20 μm. (b) Using nanofibers as a carrier prolonged the drug retention inside the cells. A comparison of the cellular uptake efficiency of the fluorescence aldox-NFP and free aldox in MDA-MB-468 cell line. Fluorescence intensity of the cell lysates was recorded 6 and 24 h after replacing the culture media containing the 2 drug formulations with fresh medium. (c) Aldox-NFP was more efficient in breaking down tumor spheroids into multiple pieces compared to Doxil (50 μM of drug content). Microscopic images showing the

morphological changes of the treated MDA-MB-468 spheroids treated over time. The scale bar is 200 μm.

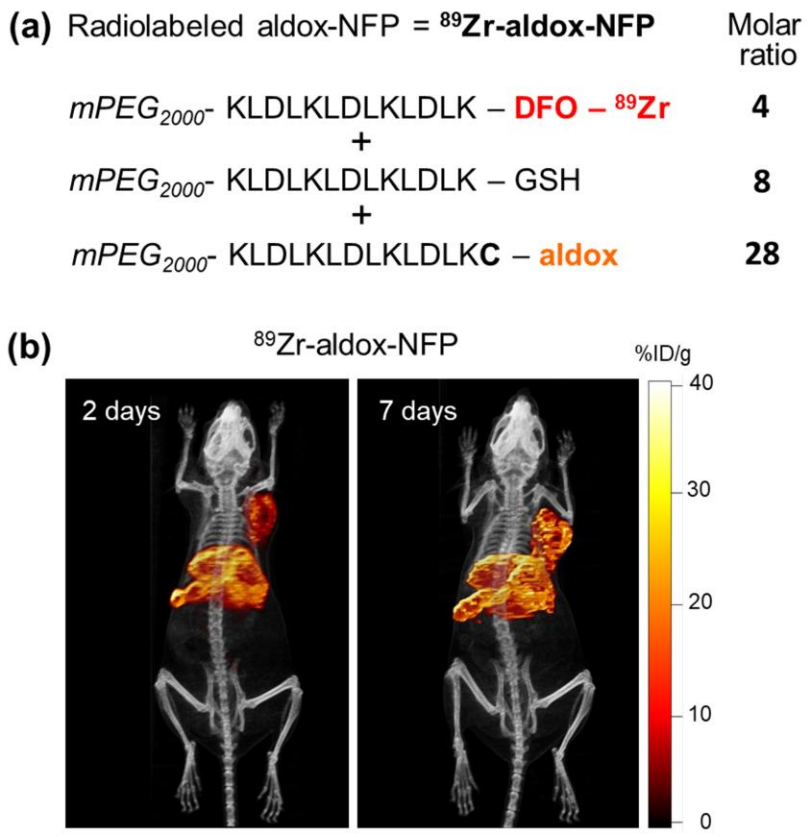

Figure S9: (a) The ratio of different peptide constructs used for assembling radiolabeled aldox-NFP (^{89}Zr-aldox-NFP). (b) PET/CT images confirmed that incorporation of aldox into GSH-NFP did not alter the tumor-preferential biodistribution. Whole body images were acquired 2 and 7 days after injection of ^{89}Zr-labeled aldox-NFP (n=4/group).

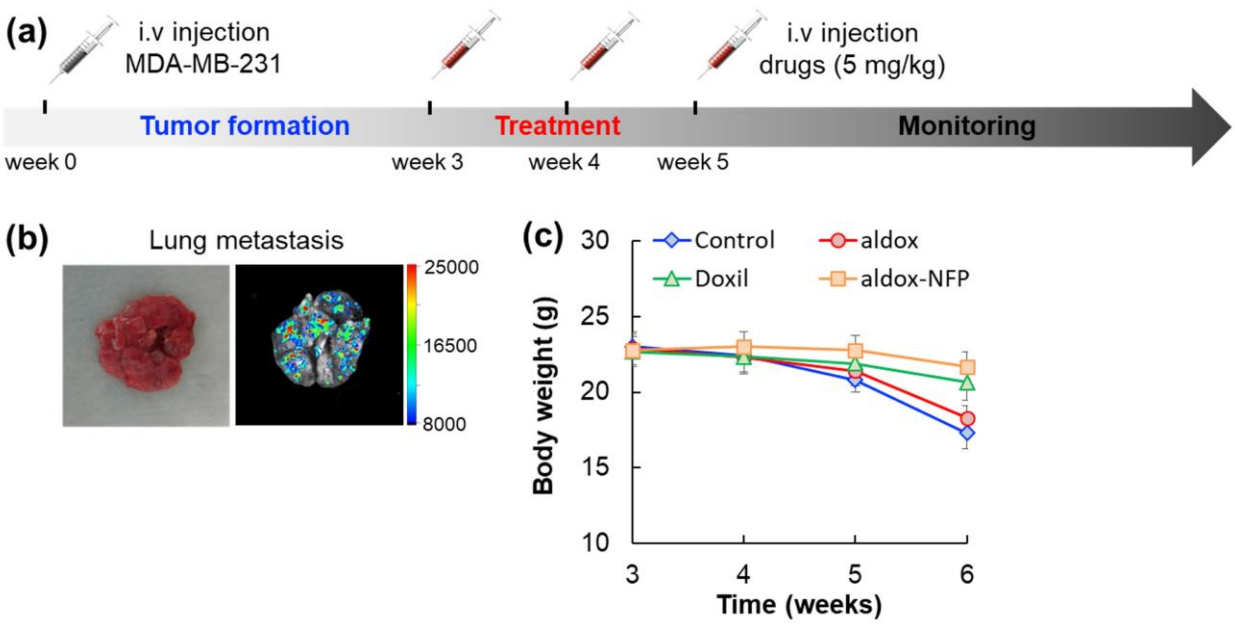

Figure S10: (a) Schematic diagram showing the dose schedule of the survival study. (b) Representative photo and GFP fluorescence image of the excised lungs bearing tumor lesions. Images were acquired three weeks after MDA-MB-231 cells inoculation. (c) Body weight changes in NSG mice bearing MDA-MB-231 lung metastasis and treated with PBS, aldox, Doxil, or aldox-NFP (5 mg/kg of drug content).